Supporting Information

Chitosan-based Magnetic Iron Oxide Nanohybrids Enabling pH-Controlled Adsorption and Release of DNA

Ankur Verma[1], Parmanand Kushwaha[1], Manisha Behera[2], Ramandeep Kaur[1], Kumari Pragya[1], Archisman Samanta[1], Sovon Acharya[3], Jaydeep Bhattacharya[4], Sachinandan De[1]*

[1]Animal Genomics Laboratory, Animal Biotechnology Division, ICAR-National Dairy Research Institute, Karnal, Haryana 132001, India

[2]Department of Zoology, Hindu College, University of Delhi, Delhi 110007, India

[3]School of Biotechnology, Amity University, Gurugram, Haryana 122412, India

[4]Nanobiotechnology Laboratory, School of Biotechnology, Jawaharlal Nehru University, New Delhi-110067, India

SI 1. Primers used in polymerase chain reaction for the amplification of *uidA* and *nuc* gene of *Escherichia coli* and *Staphylococcus aureus* respectively.

Target organism	Gene (primer)	Sequence (5′→3′)	Tm (°C)	Product size
E. coli	*uidA* (Forward)	TGGCAGGTGGTGGCAAA TGGTGGTG	60	200 bp
	uidA (Reverse)	CCGACGCGCAGCGGGTA GATAT		
S. aureus	*nuc* (Forward)	GATGGCTATCAGTAATG TTTCGAAAGGGC	60	516 bp
	nuc (Reverse)	ACATAAGCAACTTTAGC CAAGCCTTGACG		

SI 2. Weight % composition of iron oxide nanoparticles (IONP) and chitosan-coated iron oxide nanoparticles (IONP@Chitosan) by EDS analysis.

Element	Description	IONP	IONP@Chitosan
Fe	Iron	63.78	75.07
C	Carbon	19.89	17.43
O	Oxygen	16.34	6.80
N	Nitrogen	-	0.70

SI 3. Atomic % composition of iron oxide nanoparticles (IONP) and chitosan-coated iron oxide nanoparticles (IONP@Chitosan) by EDS analysis.

Element	Description	IONP	IONP@Chitosan
Fe	Iron	29.90	41.11
C	Carbon	43.36	44.37
O	Oxygen	26.74	13.00
N	Nitrogen	-	1.52

SI 4. Dynamic light scattering (DLS) measurements of uncoated iron oxide nanoparticles (IONPs) and chitosan-coated iron oxide nanoparticles (IONP@Chitosan). Individual replicate values (n = 3) and corresponding mean ± standard deviation (SD) are presented for hydrodynamic diameter (Z-average) and polydispersity index (PDI).

Sample	Z-Average (d. nm)	Polydispersity Index (PDI)	Mean ± SD (Size)	Mean ± SD (PDI)
IONP	**175.4**	**0.285**	**175.9 ± 7.0**	**0.324 ± 0.040**
	169.1	**0.321**		
	183.1	**0.365**		
IONP@Chitosan	**271.6**	**0.201**	**283.3 ±10.2**	**0.275 ± 0.064**
	290.3	**0.307**		
	288.0	**0.317**		

SI 5. Zeta potential measurements of uncoated iron oxide nanoparticles (IONPs) and chitosan-coated iron oxide nanoparticles (IONP@Chitosan). Individual replicate values (n = 3) and corresponding mean ± standard deviation (SD) are presented.

Sample	Z-Potential (mV)	Mean ± SD (Zeta)
IONP	**6.20**	**7.51 ± 1.15**
	8.37	
	7.95	
IONP@Chitosan	**38.2**	**38.9 ± 1.82**
	37.5	
	41.0	

SI 6. Adsorption and desorption of genomic DNA of *Escherichia coli* and *Staphylococcus aureus* on uncoated iron oxide nanoparticles (IONPs) and chitosan-coated iron oxide nanoparticles (IONP@Chitosan).

Bacterial Species	Initial DNA Input (µg)	Nanoparticle Type	Adsorbed DNA (%)	Desorbed DNA (µg)	Desorption Efficiency (%)
E. coli	50.7	IONP	39.4	4.1	8.1
		IONP@Chitosan	92.8	38.5	76.8
S. aureus	43.0	IONP	36.3	3.6	8.4
		IONP@Chitosan	90.5	31.5	75.9

SI 7. The concentration of DNA in the adsorption-desorption process was measured quantitatively using uncoated iron oxide nanoparticles (IONP) and chitosan-coated iron oxide nanoparticles (IONP@Chitosan) with genomic DNA of *Escherichia coli* (I) and *Staphylococcus aureus* (II). The reduction in DNA levels after adsorption and a large amount of recovery in the elution fractions are evidence of the high DNA-binding and release efficiency of IONP@Chitosan as compared to that of bare IONP. s = stock DNA (initial input); b_1, w_1, e_1 = binding supernatant, wash, and elution fractions of IONP; b_2, w_2, e_2 = binding supernatant, wash, and elution fractions of IONP@Chitosan.

Sample	Concentration (ng/ µl)
Stock DNA (s)	507.4
Binding Solution (b_1)	307.4
Washing Solution (w_1)	70.7
Elution Solution (e_1)	20.9
Binding Solution (b_2)	36.3
Washing Solution (w_2)	-1.0*
Elution Solution (e_2)	389.9

(I)

Sample	Concentration (ng/ µl)
Stock DNA (s)	430.5
Binding Solution (b_1)	265.3
Washing Solution (w_1)	59.6
Elution Solution (e_1)	11.2
Binding Solution (b_2)	40.8
Washing Solution (w_2)	-3.5*
Elution Solution (e_2)	323.2

(II)

*Washing fractions which have negative value are the artifacts of NanoDrop baseline correction and reflects that the DNA concentration was below the detection limit.

SI 8. Ultraviolet (UV) spectra of genomic DNA of *Escherichia coli* were measured prior to adsorption (control), following adsorption and following desorption. **Left:** uncoated iron oxide nanoparticles (IONP) were partially adsorbed and DNA could not be recovered completely, only 41.3 ng/µL DNA eluted. **Right:** DNA desorption was much higher in chitosan-coated iron oxide nanoparticles (IONP@Chitosan) with 389.9 ng/µL DNA obtained. These results are in line with the gel electrophoresis results in **Figure 6(a)**.

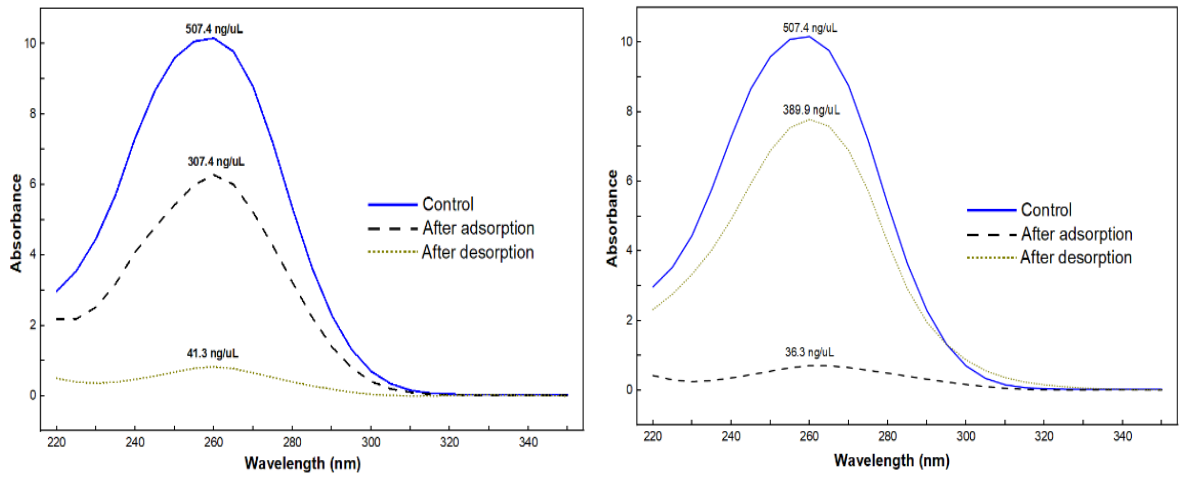

SI 9. Ultraviolet (UV) spectra of genomic DNA of *Staphylococcus aureus* were measured prior to adsorption (control), following adsorption and following desorption.

Left: when the iron oxide nanoparticles (IONPs) were not coated, the DNA yield was low with only 36.4 ng/µL of DNA eluted. **Right:** chitosan-coated iron oxide nanoparticles (IONP@Chitosan) have showed higher DNA desorption and 323.2 ng/µL DNA is obtained. The gel electrophoresis results outcomes and findings indicated in **Figure 6(b)** are supported by these observations.

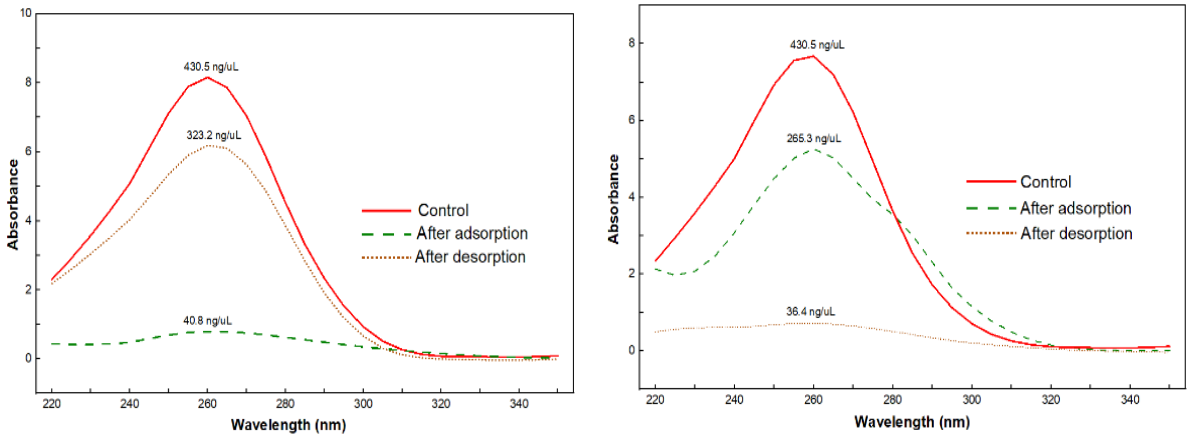

SI 10. DNA yield and purity ratios of genomic DNA of *Escherichia coli* and *Staphylococcus aureus* using uncoated iron oxide nanoparticles (IONPs) and chitosan-coated iron oxide nanoparticles (IONP@Chitosan).

Bacterial Species	Nanoparticle Type	DNA Yield (ng/µL)	$A_{260/280}$ Ratio	$A_{260/230}$ Ratio
E. coli	IONP	14.3	1.46	1.10
	IONP@Chitosan	170.9	1.95	2.70
S. aureus	IONP	22.2	2.70	4.70*
	IONP@Chitosan	153.6	1.86	2.72

SI 11. Ultraviolet-visible (UV-Vis) spectrum of *Escherichia coli* genomic DNA **(I)** and *Staphylococcus aureus* genomic DNA **(II)** indicated increased absorbance at 260 nm with the use of chitosan-coated iron oxide nanoparticles (IONP@Chitosan) in comparison to the uncoated iron oxide nanoparticles (IONP) consistent with higher DNA recovery**.**

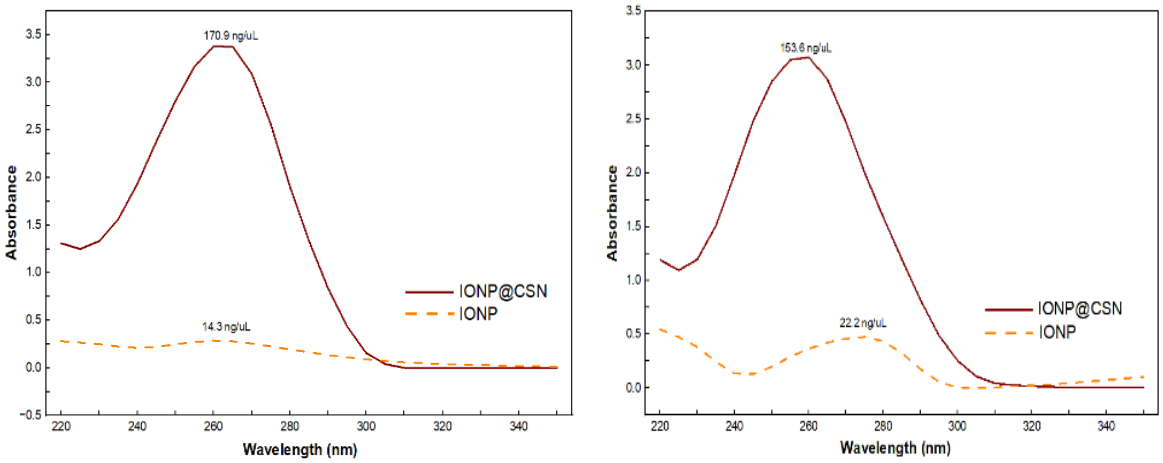

(I) **(II)**

SI 12. Schematic illustration of β-(1→4)-linked chitosan-mediated functionalization of iron oxide nanoparticles and electrostatic interaction between protonated amine groups ($-NH_3^+$) and the phosphate backbone of bacterial genomic DNA under acidic conditions.

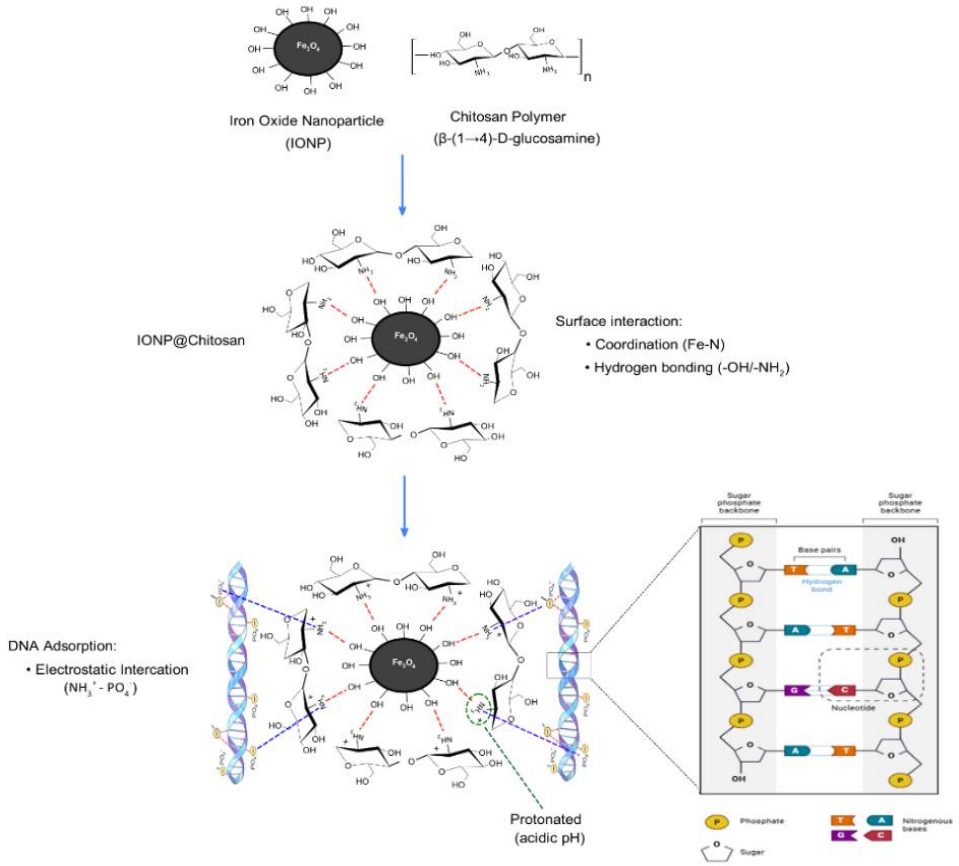

SI 13. Comparison of the adsorption and desorption capacity of the DNA on chitosan-coated iron oxide nanoparticles with the reported magnetic DNA adsorbents emphasizing on pH conditions, contact time, and extraction efficiency.

Surface Functionalization	DNA Adsorbed	pH	Adsorption time (min)	Adsorption Efficiency (%)	Desorption time (min)	Desorption Efficiency (%)	Ref.
Mesoporous silica	*Salmon sperm*	7.6	20	83	60	89.5	[1]
Hemoglobin	*Plasmid*	6.1	15	68.3	15	68.3	[2]
Bromoacetic acid/acridine	*Plasmid*	6.2	15	88	-	-	[3]
Montmorillonite	*Salmon sperm*	2.0 - 5.0	30	72	140	46.6	[4]
Polyethyleneimine	*Salmon sperm*	4.0	20	70	5	70.0	[5]
Zirconia	*Tobacco*	2.0	20	85	5	81.3	[6]
Polydopamine	*Calf thymus*	2.0	10	90	10	-	[7]
1-hexyl-3-methylimidazolium bromide	*Herring sperm*	3.0	20	85	30	96.0	[8]
Chitosan-Nanotube-PEG	*Salmon sperm*	4.0	15	88	-	79.0	[9]
Au - Polyethyleneimine	*Salmon sperm*	5.0	20	83	20	87.0	[10]
Zirconia phosphonates	*Salmon sperm*	-	30	92	240	89.0	[11]
PSG-NH_2-SiO_2	*Plasmid*	5.0	20	80	-	56.3	[12]
Polyaniline Polypyrrole	*Aspergillus niger*	-	10	96	40 - 60	-	[13]
Polyaniline	*Salmon sperm*	3.8	10	92	2	96.5	[14]
Chitosan-Polyaniline	*Salmon sperm*	3.6	10	98	-	66.0	[15]
PEDOT	*Salmon sperm*	2.5	10	60	5	94.2	[16]
Chitosan	***E. coli*/*S. aureus***	**3.2**	**5**	**92.8/90.5**	**5**	**76.8/75.9**	**This work**

SI 14. Uncropped gel imgaes.

(a) Full-length uncropped agarose gel corresponding to **Figure 6(a)** showing genomic DNA adsorption and desorption by uncoated iron oxide nanoparticles (IONP) and chitosan-coated iron oxide nanoparticles (IONP@Chitosan) using *Escherichia coli* genomic DNA. Lanes: s, stock DNA; b_1 and b_2, binding supernatants; w_1 and w_2, wash fractions; e_1 and e_2, elution fractions.

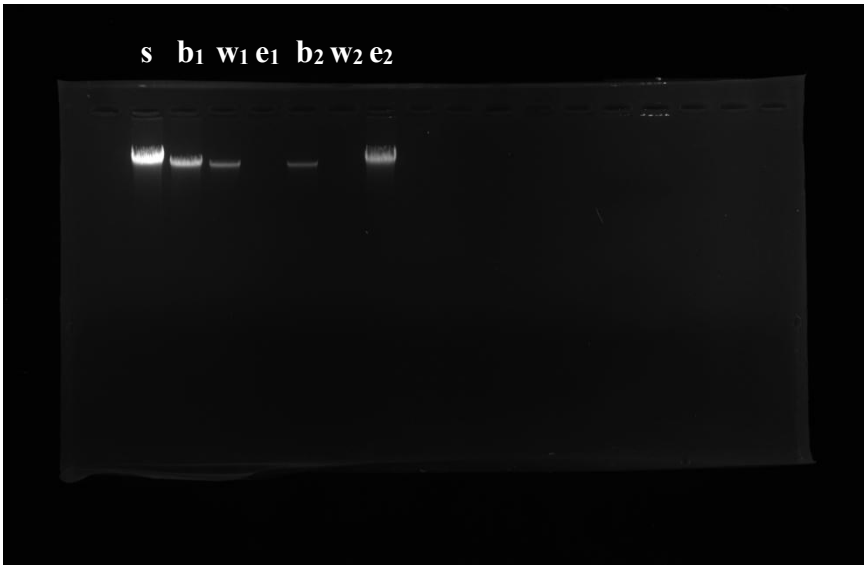

(b) Full-length uncropped agarose gel corresponding to **Figure 6(b)** showing genomic DNA adsorption and desorption by uncoated iron oxide nanoparticles (IONP) and chitosan-coated iron oxide nanoparticles (IONP@Chitosan) using *Staphylococcus aureus* genomic DNA. Lanes: s, stock DNA; b_1 and b_2, binding supernatants; w_1 and w_2, wash fractions; e_1 and e_2, elution fractions.

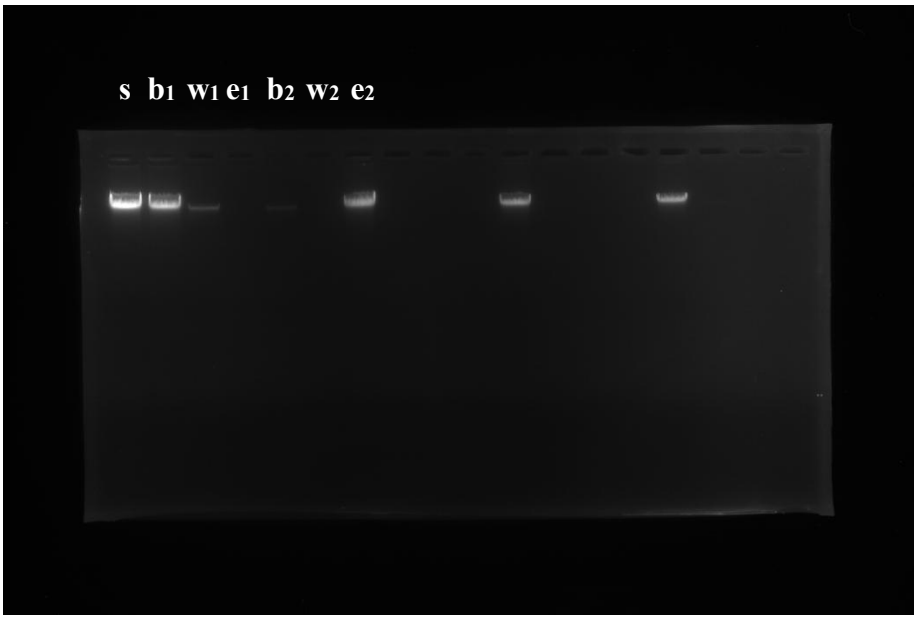

(c) Uncropped agarose gel corresponding to **Figure 7(a)** showing genomic DNA isolated from *Escherichia coli* using uncoated iron oxide nanoparticles (IONPs) and chitosan-coated iron oxide nanoparticles (IONP@Chitosan). Lanes N_1 and N_2 represent negative controls. Lane E_1 corresponds to DNA isolated using uncoated IONPs, whereas lane E_2 corresponds to DNA isolated using IONP@Chitosan.

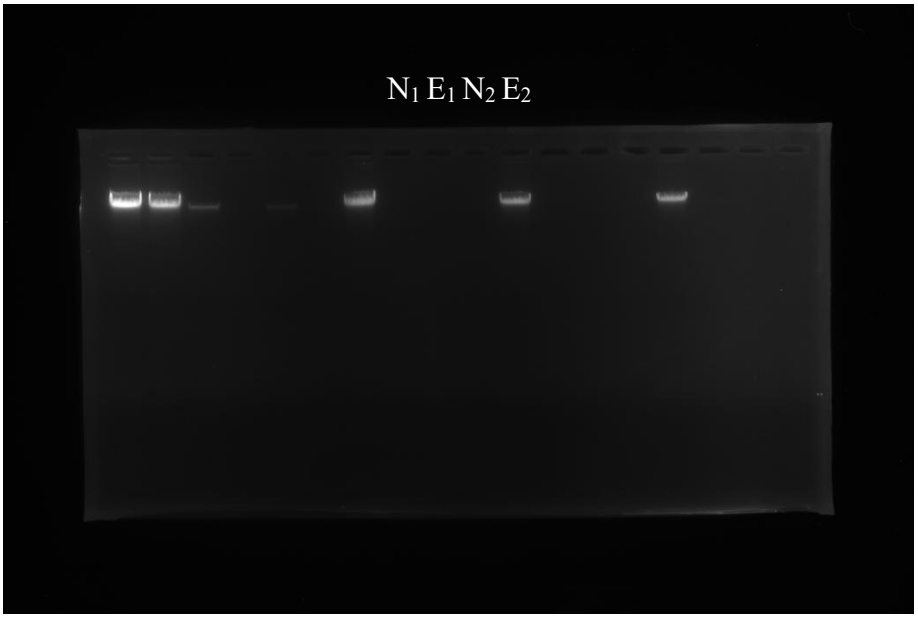

(d) Uncropped agarose gel corresponding to **Figure 7(b)** showing genomic DNA isolated from *Staphylococcus aureus* using uncoated iron oxide nanoparticles (IONPs) and chitosan-coated iron oxide nanoparticles (IONP@Chitosan). Lanes N_1 and N_2 represent negative controls. Lane S_1 corresponds to DNA isolated using uncoated IONPs, whereas lane S_2 corresponds to DNA isolated using IONP@Chitosan.

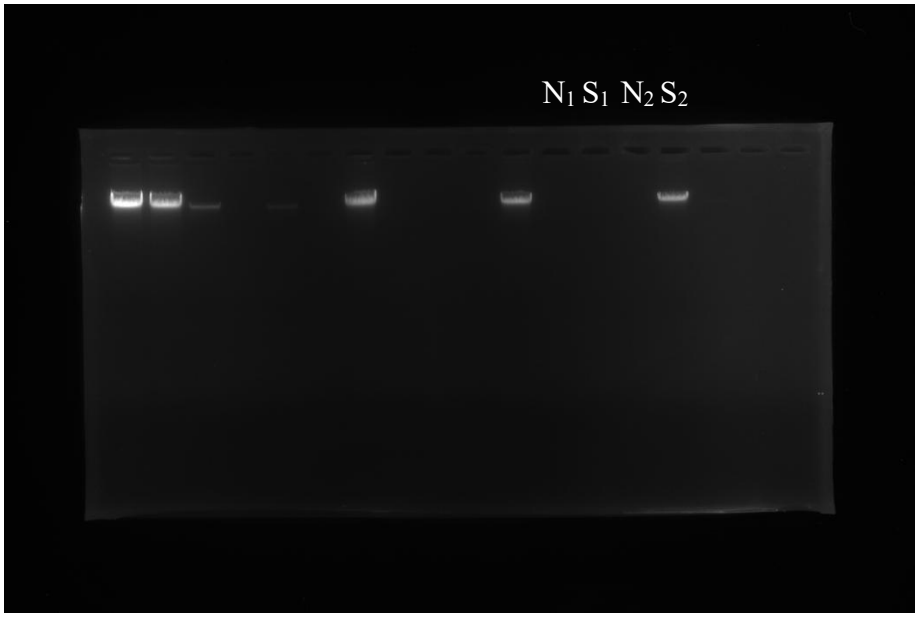

(e) Full-length uncropped agarose gel corresponding to **Figure 8(I)** showing PCR amplification of the *uidA* gene from *Escherichia coli* genomic DNA isolated using iron oxide nanoparticles (IONP) and chitosan-coated iron oxide nanoparticles (IONP@Chitosan). Additional lanes visible in the gel correspond to unrelated samples analyzed on the same gel and were not included in **Figure 8(I)**.

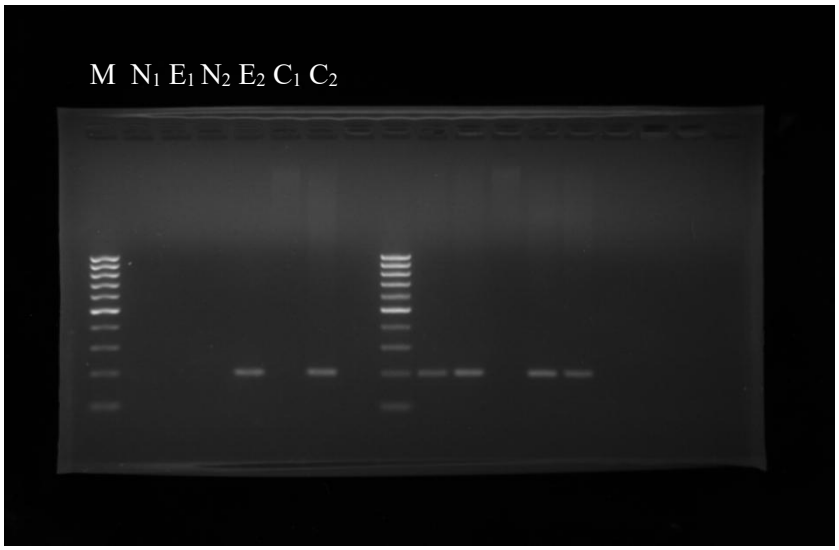

(f) Full-length uncropped agarose gel corresponding to **Figure 8(II)** showing PCR amplification of the *nuc* gene from *Staphylococcus aureus* genomic DNA isolated using iron oxide nanoparticles (IONP) and chitosan-coated iron oxide nanoparticles (IONP@Chitosan). Additional lanes visible in the gel correspond to unrelated samples analyzed on the same gel and were not included in **Figure 8(II)**.

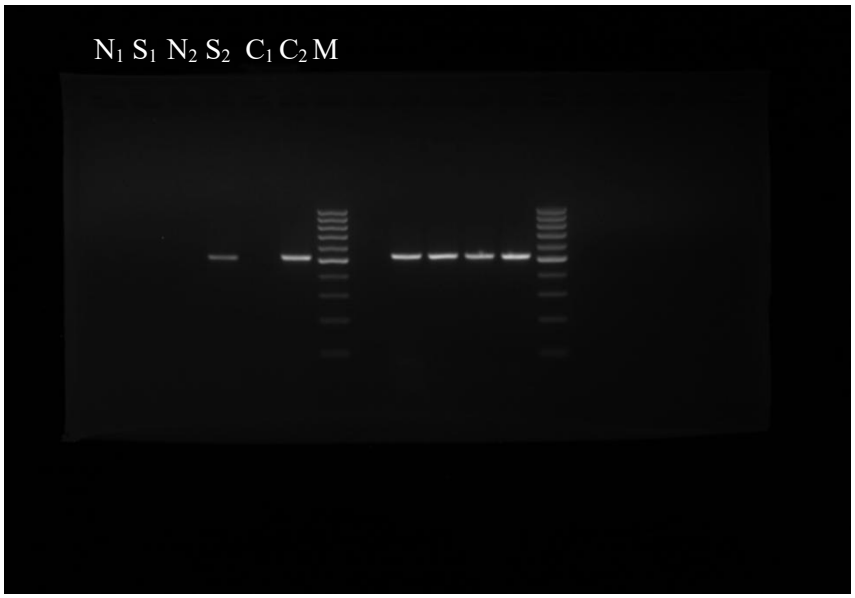

REFRENCES

[1] X. Li, J. Zhang, H. Gu, Adsorption and Desorption Behaviors of DNA with Magnetic Mesoporous Silica Nanoparticles, *Langmuir*, 27 (2011) 6099-6106.

[2] X.-W. Chen, Q.-X. Mao, J.-W. Liu, J.-H. Wang, Isolation/separation of plasmid DNA using hemoglobin modified magnetic nanocomposites as solid-phase adsorbent, Talanta, 100 (2012) 107-112.

[3] S.L. Sahoo, C.-H. Liu, Adsorption behaviors of DNA by modified magnetic nanoparticles: Effect of spacer and salt, Colloids and Surfaces A: Physicochemical and Engineering Aspects, 482 (2015) 184-194.

[4] P. Cai, Q. Huang, X. Zhang, H. Chen, Adsorption of DNA on clay minerals and various colloidal particles from an Alfisol, Soil Biology and Biochemistry, 38 (2006) 471-476.

[5] L.-L. Hu, B. Hu, L.-M. Shen, D.-D. Zhang, X.-W. Chen, J.-H. Wang, Polyethyleneimine–iron phosphate nanocomposite as a promising adsorbent for the isolation of DNA, Talanta, 132 (2015) 857-863.

[6] M. Saraji, S. Yousefi, M. Talebi, Plasmid DNA purification by zirconia magnetic nanocomposite, Analytical Biochemistry, 539 (2017) 33-38.

[7] Y. Wang, X. Ma, C. Ding, L. Jia, pH-responsive deoxyribonucleic acid capture/release by polydopamine functionalized magnetic nanoparticles, Analytica Chimica Acta, 862 (2015) 33-40.

[8] M. Ghaemi, G. Absalan, Study on the adsorption of DNA on Fe_3O_4 nanoparticles and on ionic liquid-modified Fe_3O_4 nanoparticles, Microchimica Acta, 181 (2014) 45-53.

[9] K. Xu, Y. Wang, H. Zhang, Q. Yang, X. Wei, P. Xu, Y. Zhou, Solid-phase extraction of DNA by using a composite prepared from multiwalled carbon nanotubes, chitosan, Fe_3O_4 and a poly(ethylene glycol)-based deep eutectic solvent, Microchimica Acta, 184 (2017) 4133-4140.

[10] H. Sun, X. Zhu, L. Zhang, Y. Zhang, D. Wang, Capture and release of genomic DNA by PEI modified Fe_3O_4/Au nanoparticles, Materials Science and Engineering: C, 30 (2010) 311-315.

[11] Y. Tang, Y. Ren, X. Shi, Bifunctional Mesoporous Zirconium Phosphonates for Delivery of Nucleic Acids, Inorganic Chemistry, 52 (2013) 1388-1397.

[12] S. Xu, X. Song, J. Guo, C. Wang, Composite Microspheres for Separation of Plasmid DNA Decorated with MNPs through in Situ Growth or Interfacial Immobilization Followed by Silica Coating, ACS Applied Materials & Interfaces, 4 (2012) 4764-4775.

[13] L. Gai, X. Han, Y. Hou, J. Chen, H. Jiang, X. Chen, Surfactant-free synthesis of Fe_3O_4@PANI and Fe_3O_4@PPy microspheres as adsorbents for isolation of PCR-ready DNA, Dalton Transactions, 42 (2013) 1820-1826.

[14] J.C. Medina-Llamas, A.E. Chávez-Guajardo, C.A.S. Andrade, K.G.B. Alves, C.P. de Melo, Use of magnetic polyaniline/maghemite nanocomposite for DNA retrieval from aqueous solutions, Journal of Colloid and Interface Science, 434 (2014) 167-174.

[15] B.G. Maciel, R.J. da Silva, A.E. Chávez-Guajardo, J.C. Medina-Llamas, J.J. Alcaraz-Espinoza, C.P. de Melo, Magnetic extraction and purification of DNA from whole human blood using a γ-Fe_2O_3@Chitosan@Polyaniline hybrid nanocomposite, Carbohydrate Polymers, 197 (2018) 100-108.

[16] da Silva, R. J., Pedro, G. C., Gorza, F. D. S., Maciel, B. G., Ratkovski, G. P., Mojica-Sanchez, L. C., Medina-Llamas, J. C., Chavez-Guajardo, A. E., & de Melo, C. P. (2021). DNA purification using a novel γ-Fe_2O_3/PEDOT hybrid nanocomposite. Analytica Chimica Acta, 1178, 338762.